Chemical Physics 388 (2011) 47–56

Contents lists available at SciVerse ScienceDirect

Chemical Physics

journal homepage: www.elsevier.com/locate/chemphys

Structure and orientation of water molecules at model hydrophobic surfaces with curvature: From graphene sheets to carbon nanotubes and fullerenes

L.M. Alarcón, D.C. Malaspina, E.P. Schulz, M.A. Frechero, G.A. Appignanesi *

Sección Fisicoquímica, INQUISUR-UNS-CONICET and Departamento de Química, Universidad Nacional del Sur, Avenida Alem 1253, 8000-Bahía Blanca, Argentina

ARTICLE INFO

Article history:
Received 10 August 2010
In final form 15 July 2011
Available online 3 August 2011

Keywords:
Hydrophobic hydration
Water
Graphene
Carbon nanotubes
Fullerenes

ABSTRACT

We study the structure and orientation of water molecules at model hydrophobic surfaces by means of molecular dynamics. We focus here on the role of geometry in water hydration by comparing the situation for a planar graphene sheet with convex surfaces with different curvature: the exterior surfaces of carbon nanotubes and fullerenes of different radii. In all cases, we find the first water hydration layer to be more structured than the bulk. Additionally, the first water layers are found to be well oriented with respect to the surface normal in a way consistent with a local Ice Ih-like structuring, but differently form the water–air interface (along the opposite direction with respect to ice Ih basal plane). We also show that as the curvature of the surface gets more pronounced, the water molecules get less structured and oriented. This monotonic loss of local structure for proximal water represents a smooth tendency whenever we deal with an extended surface. However, when the surface becomes partially or completely non-extended (within the sub-nanometric regime), the surface water layer becomes to quickly lose structuring and orientation.

1. Introduction

The comprehension of the structure and behavior of water at interfaces represents an issue of major concern in several central research areas like hydration, reaction dynamics and biology [1–7]. Regarding biology, water is known to play a dominant role in the structuring, the dynamics and the functionality of biological molecules [1–7]. Thus, main processes like protein folding, protein binding and biological function claim for a molecular understanding of hydration. A simple case study in this direction is the investigation of the hydration properties of model surfaces, and homogeneous hydrophobic-like surfaces are of interest. Such studies where geometry plays a main role can also be regarded as a simple first step towards more complex situations where chemistry is also at play, like the situation encountered for the so-called biological water [8], that is, the hydration water around proteins and other biological molecules. For example, graphite-like surfaces have been employed to computationally investigate the hydrophobic effect [5]. To this end [5], two parallel water confining surfaces separated by short distances have been used to determine the behavior of the contained water and the possible de-wetting effect that should mark the hydrophobic interaction [1,2,5,7]. Other hydrophobic surfaces have been studied as well (see for example [1,2,5,7,9–13] and references therein). Extended hydrophobic-like surfaces disrupt the hydrogen bond network of water. The water molecules close to the surface would lack a hydrogen bond in the direction towards the surface (as has been shown for example for an extended homogeneous flat graphene sheet [14]), thus diminishing their local connectivity from preferentially four to preferentially three first neighbors, a fact that would imply an enthalpy rise. However, this cost is in part compensated by the improvement in the remaining interactions, so that the molecules of the first hydration layers become better structured than the bulk as they tend to lower their local density [14].

In the present work we shall study by means of molecular dynamics (MDs) simulations the structure and also the orientation of the water molecules at graphene, single walled carbon nanotube and fullerene surfaces. In all cases, a better structuring than the bulk and clear preferential orientation will be evident. The study of the orientation of the water molecules is interesting since it can be directly contrasted with experimental measurements (surface sum-frequency vibrational spectroscopy [15]), when available. Additionally, we shall learn that the orientation of the water molecules at these hydrophobic surfaces is different from the one that occurs at the water–air interface. Another goal of our present work is to examine the role played by the curvature of the hydrophobic surface. Thus, we shall investigate the hydration layers of nanotubes and fullerenes of different radii. We shall focus on the convex surfaces, that is, the exterior surfaces (water confined within nanotubes and fullerenes has been extensively studied [16–18]). Our aim is to learn whether curvature affects the structuring and orientation of the hydration layers. Of particular interest is the situation when the surface becomes partially or completely non-ex-

* Corresponding author.
E-mail address: appignan@criba.edu.ar (G.A. Appignanesi).

0301-0104/$ - see front matter © 2011 Elsevier B.V. All rights reserved.
doi:10.1016/j.chemphys.2011.07.019

tended. We shall demonstrate that in the case of an extended surface, the introduction of curvature implies a slight decrease of this (better than the bulk) structuring and orientation of the molecules close to the interface. However, when the surface becomes non-extended (within the subnanometric regime), this local order of the water molecules begins to be quickly lost.

2. Methodology

2.1. Model systems

As model hydrophobic surfaces we employed a graphene sheet, single walled carbon nanotubes of different radii and C_{60} and C_{20} fullerenes. Given the chemical similarity between the three kinds of systems under study, the hydration of the graphene sheet should constitute the limit of infinite curvature radius for both the nanotubes and the fullerenes. The water molecules were modeled by the TIP3P model [19,20]. A Berendsen thermostat was used in the equilibration [21]. All simulations were done using the AMBER10 molecular simulation suite [22] with a 1 fs time step. We used the GAFF (Generalized Amber Force field) and FF99SB force fields for carbon and water, respectively (the atom type in GAFF is *ca* for carbon and *ha* for hydrogen atom). The default water model for the FF99SB force field is TIP3P, and thus the different parameters are optimized for this case. All calculations were performed in the NPT ensemble with a Langevin thermostat. The model graphene surface was a perfect honeycomb graphite-like sheet, consisting of a layer of 5 by 5 benzenic rings (approximately 100 Å^2) with terminations in hydrogen atoms solvated with 4365 TIP3P water molecules in an orthogonal cubic box with periodic boundaries [14]. The surface was centered in the middle of the box and parallel to the XY plane. To discard the presence of significant finite size effects (see below) we also employed a second layer of 10 by 10 benzenic rings (approximately 400 Å^2), solvated with 10,788 TIP3P water molecules. In order to avoid molecules close to borders of the graphite sheet, we considered a circular tube of radius 4.8 Å (8.4 Å for the larger system) placed at the center of the graphite layer and normal to such plane. We then divided the tube in six consecutive regions or cylinders (from region or cylinder 1 to region or cylinder 6) of height 3.5 Å so that the first cylinder extended from the surface to a distance of 3.5 Å, the second one went from 3.5 Å to 7 Å, and so on. This distance implies that the first region contained water molecules exclusively from the first peak of the water density distribution function normal to the surface [14]. Since the system is equivalent in the two directions normal to the graphite plane, we gathered statistical data from both sides of the sheet (that is, we also constructed a tube normal to the graphite sheet but extending to the other direction and divided it into six cylinders). Thus, from now on when we speak of a given region or cylinder number it means that we are gathering data from the water molecules of the corresponding cylinders at the two sides of the graphite layer. We have previously studied the structuring of the water molecules for these graphene sheets (see details in [14]), but have not studied the orientation of the water molecules in such work. Thus, in the present work we shall focus on the orientational study of the water molecules around the graphene sheet and, for completeness, we shall also present the relevant data on the local structure of the water molecules.

In turn, the carbon nanotubes employed had radii 2.0, 3.9, 4.75, 8.15, 12.25, 20.4 and 67.5 Å. Each of the nanotubes was solvated in a box of TIP3P water molecules that extended more than 20 Å away from the nanotube borders in each direction. The axis of the nanotube coincided with the *x* axis and the length of the nanotubes was 14 Å in all cases and thus, this dimension was always extended. We studied the water molecules located within six concentric annular regions of 3.5 Å thickness so that the first region contained the water molecules external to the nanotube whose distance to the nanotube surface within the (y,z) plane at its corresponding *x* value was lower than 3.5 Å, the second region involved the molecules whose distance to the surface lay between 3.5 Å and 7 Å, and so on. In other words, we divided the region external to the nanotube into six concentric tubes (the first tube radius was 3.5 Å larger than that of the nanotube, the second one's radius was 7 Å larger than the nanotube, and so on) and the region defined by any given tube excluded the molecules within all the previous ones. In all cases, the regions studied were more than 2 Å apart from the nanotube *x*-endings in order to avoid border effects.

Finally, the fullerenes studied were C_{60} and C_{20} and were centered at the center of coordinates. Both of them were also solvated in a box of TIP3P water molecules that extended more than 20 Å away from the fullerene surface. We also studied water molecules within six regions. The spherically concentric regions studied were such that the region 1 contained the water molecules external to the fullerene whose distance to its surface was less than 3.5 Å, the second one involved water molecules whose distance to the fullerene lied between 3.5 Å and 7 Å, and so on.

In all cases we carried simulations at a temperature of 300 K (unless we explicitly indicate another value), mean pressure of 1 bar and average density around 1.0 kg/dm^3. We used a time step of 1 fs and a long range interaction cutoff of 8 Å with particle mesh Ewald. Equilibration was tested by monitoring the behavior of thermodynamical properties like temperature, pressure and energy oscillations, and by dynamical properties like oscillations in the mean squared displacement of the water molecules; the equilibration times were in each case much larger than the structural relaxation time, τ_α, for pure water at this temperature (τ_α is the timescale when the self-intermediate scattering function evaluated at the first peak of the structure factor has decayed to $1/e$).

2.2. Local structural index

Liquid water is known to present several anomalies which become more prominent as it is supercooled [23–26]. Such anomalies have been tentatively associated to structural facts: the presence of two competing preferential local structures, identified with molecules characterized by high or low local density [24,27,28]. Support for this idea comes from the existence of at least two different forms of amorphous glass states, namely low-density amorphous ice and (very) high-density amorphous ice [29–32]. Different parameters have been proposed to study the local structural order of the water molecules on a quantitative basis. One of them, proposed by Shiratani and Sasai [27,28], associates a local structure index I to each molecule to quantify the degree of local order. The key observation is the existence of certain molecules which show an unoccupied gap between .2 Å and 3.8 Å in their radial-neighbor distribution for certain periods of time. Such low-density molecules are well structured and coordinated in a highly tetrahedral manner with four other water molecules. Occupancy of such gap increases the local density and distorts the tetrahedral order of the central molecule. Shiratani and Sasai [27,28] defined $I(i,t)$ for molecule i at time t. For each molecule i one orders the rest of the molecules depending on the radial distance r_j between the oxygen of the molecule i and the oxygen of molecule j : $r_1 < r_2 < r_j < r_{j+1} < \cdots < r_{n(i,t)} < 3.7$ Å $< r_{n(i,t)+1}$. Then, the local structure index, LSI, which we denote with $I(i,t)$ is defined as [27,28]:

$$I(i,t) = \frac{1}{n(i,t)} \sum_{j=1}^{n(i,t)} [\Delta(j;i,t) - \overline{\Delta}(i,t)]^2$$

where $\Delta(j;i,t) = r_{j+1} - r_j$ and $\overline{\Delta}(i,t)$ is the average over all molecules of $\Delta(j;i,t)$. Thus, $I(i,t)$ expresses the inhomogeneity in the radial dis-

tribution within the sphere of radius around 3.7 Å. A high value of $I(i,t)$ implies that molecule i at time t has a good tetrahedral local order and low local density (and thus, a low local potential energy since it is able bind to its first four neighbors by geometrically well-shaped hydrogen bonds), while on the contrary, values of $I(i,t) \approx 0$ indicate a molecule with defective tetrahedral order and high-local density (and thus, high local potential energy), even allowing for a fifth neighbor within the coordination shell. This abnormal coordination could also promote the formation of bifurcated hydrogen bonds (when a water molecule binds to two others via the same hydrogen), a feature that has been shown to promote local mobility [33,34]. Liquid water both in the normal liquid state and in the supercooled liquid state has been shown to present local structural index distributions with a peak at low values and a tail to the right. Over certain temperature range the curves for the different temperatures intersect at a value of $I(i,t) \approx 0.04$ Å^2, which can be regarded as a limit between structured (the ones with $I(i,t) > 0.04$ Å^2) and unstructured water molecules (with values of the local structural index lower than such threshold). The fraction of structured molecules increases as temperature is decreased [27,28,35]. In a previous work for pure water [35] we have employed the inherent dynamics formalism (which implies minimizing each instantaneous configuration of the MD simulation, that is, the one for the real dynamics, to reach the basin of attraction or local minimum of the potential energy to which it belongs; that is, by subtracting the kinetic energy). This procedure renders a local structural index distribution clearly bimodal, with a kind of isosbestic point or local minimum in the distribution whose position is temperature independent, separating two peaks: the one for the unstructured molecules (to the left) and the one for the structured ones (to the right) [35]. However, in this work we shall employ directly the real dynamics to characterize the local structure of the water molecules since it suffices to this end and thus there is no need to resort to the more computationally involved inherent dynamics technique. Additionally, we note that the local structure index yields similar information on bulk water as other quantities that have been calculated, like the orientational order parameter q, which depends on the values of the angles between the lines connecting the oxygen of a given molecule with those of its nearest neighbors [36,35]. However, while the local structure index can be directly employed for water

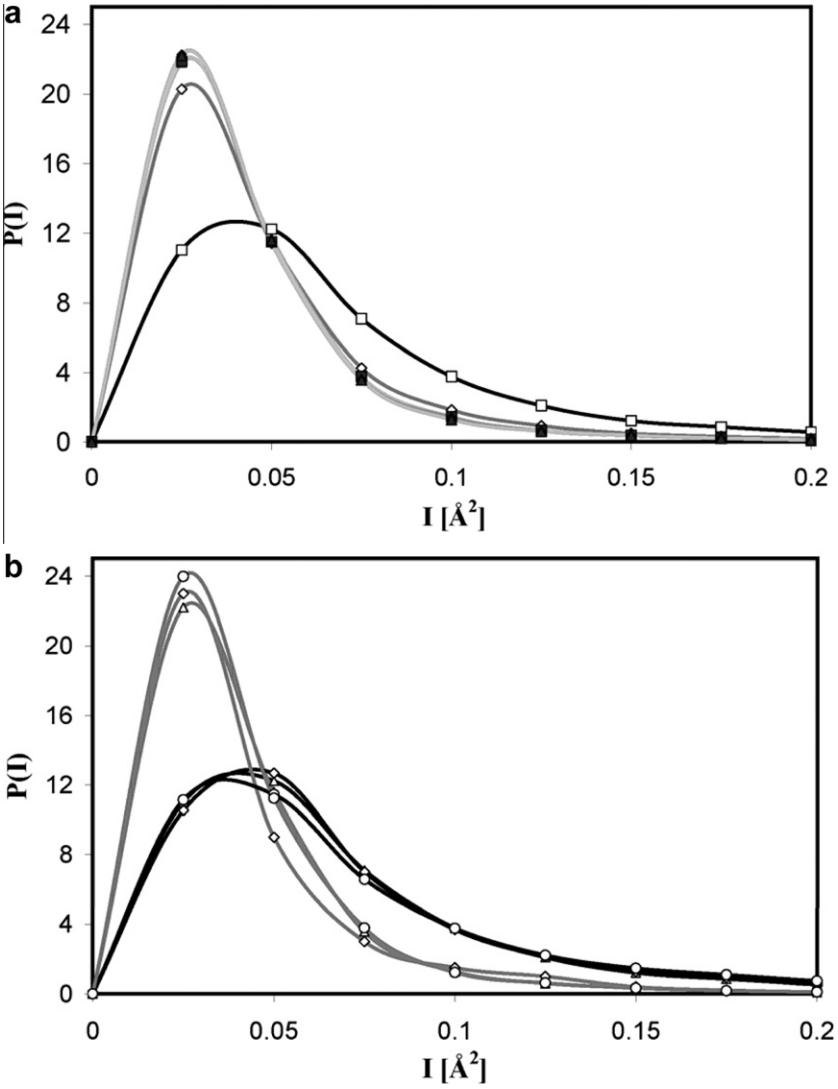

Fig. 1. (a) Probability density $P(I)$ of finding a molecule with local structure index I for each of the six regions or cylinders around the graphene sheet at temperature 300 K. The curve for cylinder 1 is depicted by open squares and the one for cylinder 2 is marked by open diamonds. The curves for cylinders 3–6 are almost coincident. Please remind that cylinder 1 contains the water molecules closest to the graphite layer while cylinder 6 comprises the studied molecules that are farther apart from it. (b) $P(I)$ for region 1 (black lines) around the graphene sheet but for different water models: TIP3P (triangles), SPC/E (diamonds) and TIP5P (circles). The gray lines display the corresponding behavior for bulk layers.

at interfaces (since it measures the quality of the local interactions of the water molecules regardless of their number), the index q cannot be used in its original form (which demands the evaluation of the positions of the first four neighbors) and should be reformulated in a nontrivial way in order to be suited for an interface [14]. The use of these kind of indices to characterize the local structure of the water molecules at an interface (instead of the study of density profiles and other parameters already used and which provide less detailed information) is also relevant since they can point to connections with dynamical quantities (for example, they have proven useful in determining the existence of a causal link between structure and dynamic propensity in glassy water, an issue of great interest in glass physics [37–39]).

3. Results and discussion

3.1. Structure of hydration water

Fig. 1(a) shows the distribution of $I(i,t)$, $P(I)$, for the water molecules within each of the six studied regions or cylinders at $T = 300$ K for the graphene sheet. The calculation of $P(I)$ for molecules within a given cylinder is performed by computing the index in many configurations that occur at different times along large runs (thus, we always employ instantaneous configurations gathering statistics from many different configurations, which warrants that all the water molecules considered reside within the region of interest). From this graph we can learn that the water molecules closest to the surface (that of region 1, that is to say, the first cylinder) are considerably better structured than the rest. In fact, all the other regions show basically the same distribution (clearly displaced to the left) except for region 2 that tends to deviate slightly from such behavior. Thus, the effect of the interface is both significant and quite local in space: The water molecules close to the surface rearrange considerably their local structure, but in less than 8 or 10 Å from the surface the water molecules are able to attain the structuring typical of the bulk (the $P(I)$ curve for pure water is in fact identical to that of region 6). To verify that this improvement in the structuring of the molecules close to the surface is not dependent on the water model used (TIP3P), we also analyzed other water models (TIP5P and SPC/E) and in both cases

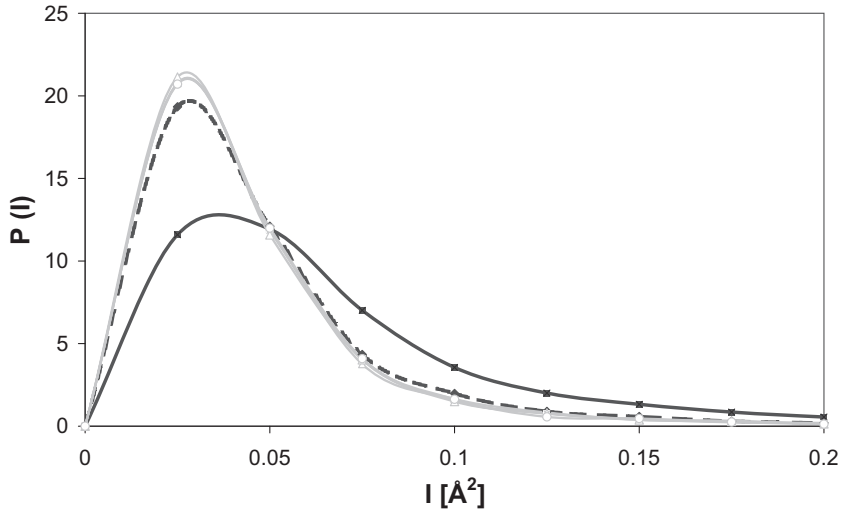

Fig. 2. Probability density $P(I)$ of finding a molecule with local structure index I for each of the six regions outside a nanotube of radius 67.5 Å at temperature 300 K. The curve for region 1 is the solid black one while that for region 2 is indicated by a dashed line. The curves for regions 3–6 are almost coincident.

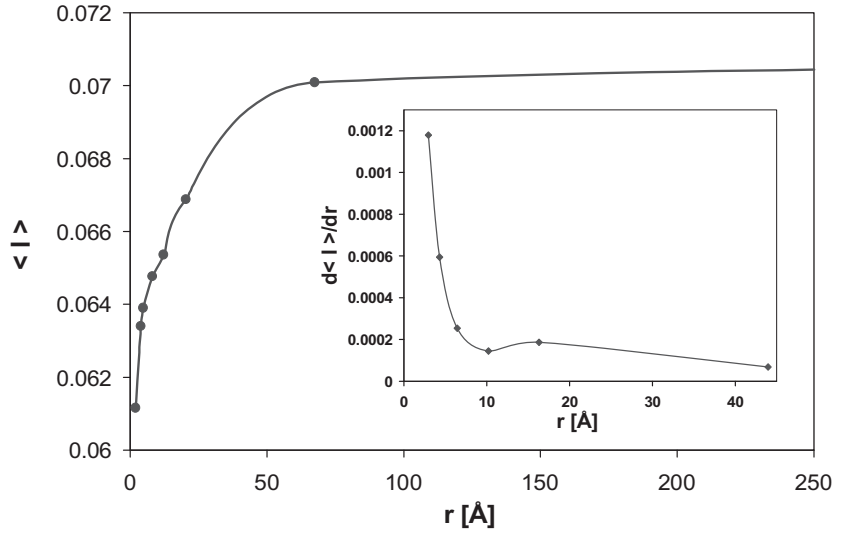

Fig. 3. Mean value of the local structure index for the molecules within the first region (region 1) external to nanotubes of different radii, as a function of the nanotube radius, r. The value corresponding to region 1 for the graphene sheet is 0.0707 Å^2. The inset shows the corresponding rate of change of the local structure index with the nanotube radius, $d\langle I\rangle/dr$. In all cases the mean value of the local structure index of the molecules within region 6 (equal to bulk water) is 0.044 Å^2.

we obtained a similar restructuring of vicinal water, as can be seen in Fig. 1(b).

In turn, Fig. 2 displays $P(I)$ for the six regions around the nanotube of radius 67.5 Å. Again we can see that the behavior of region 1 significantly deviates from the rest (also the curves for cylinders 3–6 are almost coincident), indicating the existence of an enhanced structural order. Again, we recall that region 1 is the first annular region (the water molecules closest to the exterior's nanotube surface, that is, the molecules outside the nanotube and within a tube of radius 3.5 Å larger than the nanotube radius), and that the larger the region number, the farther this region lies from the nanotube's surface.

As already pointed out and in order to study the effect of curvature on the hydration properties, we also studied nanotubes of different radii. Again, in all cases we found that only the first region around the nanotube is significantly better structured than bulk water (data not shown). For all nanotubes, we checked that the behavior for their external regions was coincident and identical to that of pure bulk water. Thus, in Fig. 3 we plot the mean value of the local structure index for region 1, $\langle I \rangle$, as a function of the nanotube radius. We also indicate the value for the graphene sheet, which could be thought as the infinite curvature radius limit. As expected, the large nanotubes display a behavior similar to that of the graphene sheet. However, we can learn that the mean I value decays smoothly but monotonically as the nanotube radius falls. Thus, the effect of curvature is to reduce the structuring of the hydrating water molecules. In turn, we present in the inset the data for the slope of such curve, that is, $d\langle I \rangle/dr$. We can easily notice that the structuring of the proximal water molecules decreases smoothly with the nanotube radius while this dimension is extended (for nanotube diameters on the nanometric range). However, a notable fact is that when this dimension becomes non-extended (diameters around and within the subnanometric size) the water molecules quickly loose structuring, with a sharp change in the curve of $d\langle I \rangle/dr$. Thus, for the small radius nanotubes we studied, the water molecules of region 1 are far less structured than the ones around the large radius nanotubes and the flat graphene sheet.

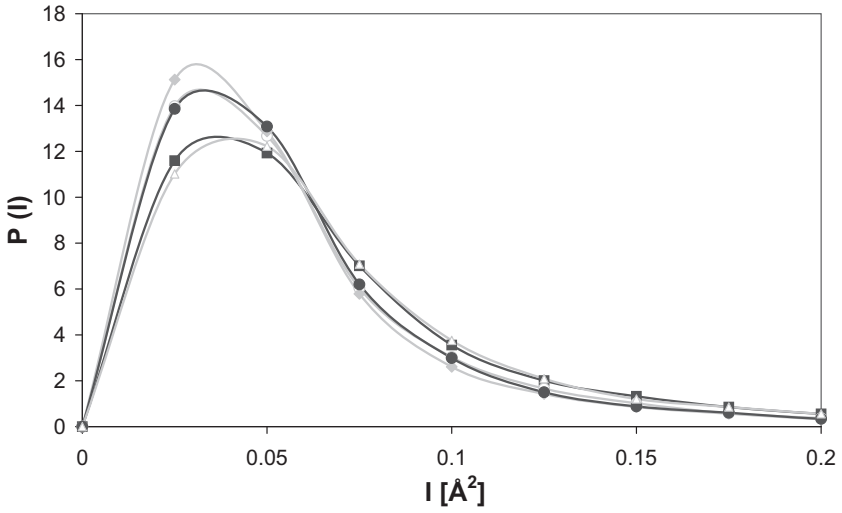

Fig. 4. $P(I)$ for the corresponding region 1 around the graphene sheet (gray line, open triangles), a nanotube of radius 67.5 Å (black line, filled squares), a nanotube of radius 2.0 Å (gray line, open circles), C_{60} (black line, filled circles) and C_{20} (gray line, filled diamonds) fullerenes.

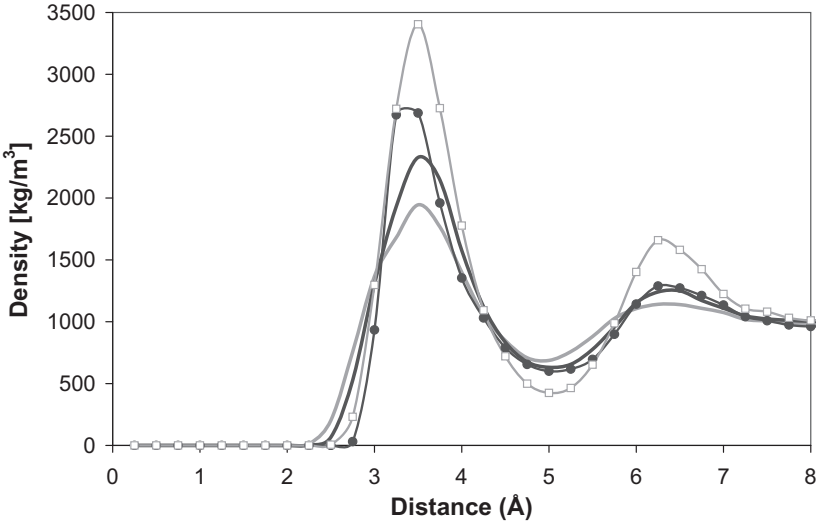

Fig. 5. Density profiles at $T = 300$ K for the water molecules as a function of their (radial) distance from the surface for graphene (black line with circles), the larger radius nanotube (black thick line) and the smaller radius nanotube (gray thick line) considered in Fig. 3. We have also included a curve for the graphene sheet at $T = 240$ K (gray line with squares) when the water molecules are much better structured as compared to the situation at $T = 300$ K.

Fig. 4 shows the probability distribution of the local structure index of region 1 for the nanotube of radius 67.5 Å, for the nanotube of radius 2.0 Å and for the fullerenes C_{60} and C_{20}, together with that for the graphene sheet. We can see that the water molecules around the small radius nanotube are far less structured than that around the large nanotube. C_{20}, which presents a completely non-extended surface (with a radius of 1.9 Å), has a water layer less structured than that of the small nanotube (surface partially non-extended, since it is in fact extended in the direction of the nanotube axis). We note that non-extended hydrophobic surfaces could be clathrated by water, as can be expected for small molecules with subnanometric dimensions. However, this is expected to happen at temperatures below water's freezing point, and simulations for molecules as small as methane or Ar_2 at such low temperatures have shown only partial clathrate tendency with very distorted configurations [40]. C_{60} is larger than C_{20} (with a radius of 3.45 Å) and its hydrating water molecules are more structured than that of C_{20}, behaving similarly to the small nanotube.

At this point, it is important to discuss in more depth this ordering effect of the vicinal water molecules (the ones closer to the surface), as indicated by the *I* index. In pure water, as temperature lowers within the liquid and in the supercooled regime, the mean value of the *I* index increases as the first two coordination layers get more compact and separate from each other (thus producing a density decrease). This exclusion of the fifth and subsequent neighbors in pure bulk water where each molecule is coordinated in a tetrahedral manner to four neighbors, improves the local order since the fifth neighbor does not disturb the structuring of the first shell. In this context, our present results indicating that the *I* index of the surface water molecules is higher than that of the bulk ones could stem from two possibilities. One of them would be a better hydrogen bonding of the molecules with their first three neighbors (we recall that at the surface the water molecules tend to be surrounded by only three first neighbors at distances compatible with hydrogen bond formation) as compared to the typical quality of bulk hydrogen bonds. Instead, such local order improvement could be due to an expanded local network comprising the fourth neighbor and the second coordination shell. We shall see that the latter explanation is in fact the correct one. We have analyzed the distances and the hydrogen bond angular orientations of the first three neighbors of the surface water molecules and determined that they are not improved with respect to that of the bulk water molecules (in fact, they are quite similar). However, the local density is indeed depleted since the fourth neighbor and, more signif-

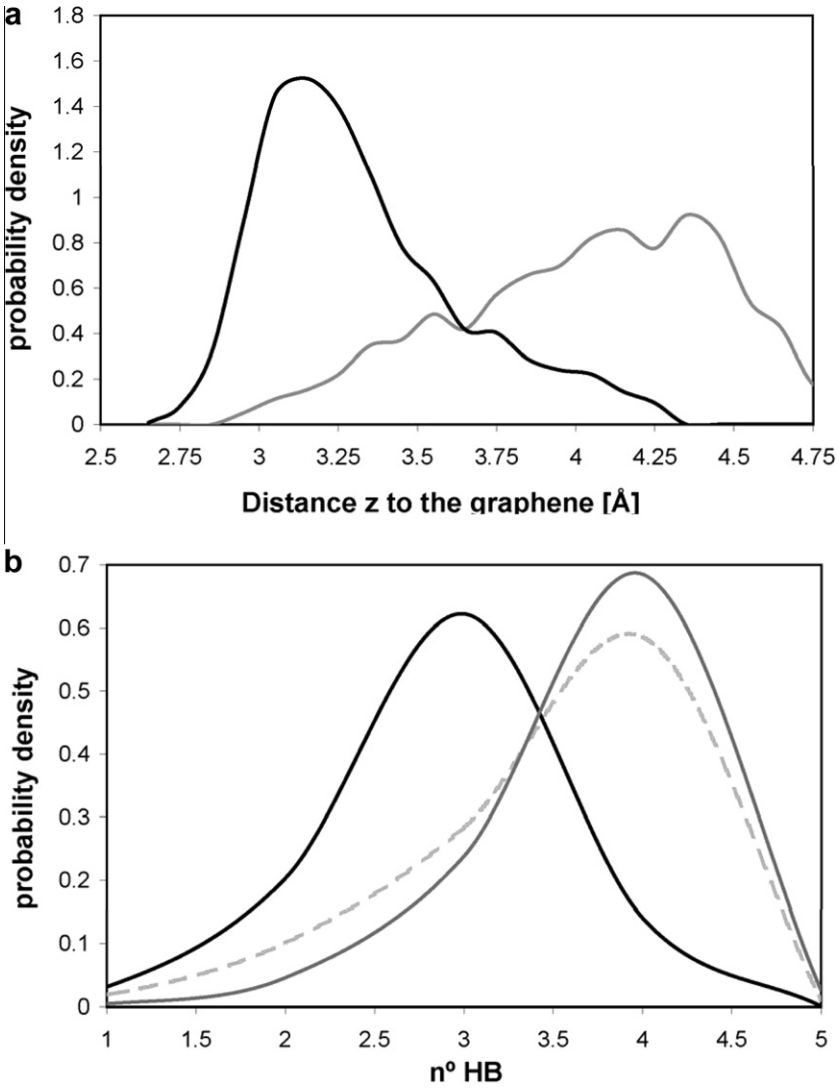

Fig. 6. (a) Probability distribution of the distance *Z* (normal to the graphene plane) at *T* = 240 K for molecules with 3 or less HBs (black curve) and molecules with 4 or more HBs (gray line) – the results are almost identical if we plot molecules with strictly 3 and molecules with strictly 4 HBs. (b) Distribution of the number of HB bonds formed by the molecules located at Layer 1 (black curve), Layer 2 (gray solid line) and for bulk molecules (molecules farther than 10 Å from the surface; dashed gray line).

icantly, the fifth neighbor are excluded away form the surface (so that their distances to the central water molecule are larger than that in bulk water). This enables a better ordering with a well developed first shell and a fourth neighbor excluded away and placed at a defined angular orientation, thus favoring OH bonds both in plane or orthogonal to the surface, as we shall demonstrate in the next subsection. We have also calculated the water density profiles as a function of the surface distance for the graphene sheet and for the small and large radius nanotubes (see Fig. 5). The graphene sheet presents the sharper distribution while the small radius nanotube shows the broader one, with increased population between the first two peaks. The peak separation enables a better local ordering, as already discussed above. We have also included the curve for the graphene sheet but at a much lower temperature

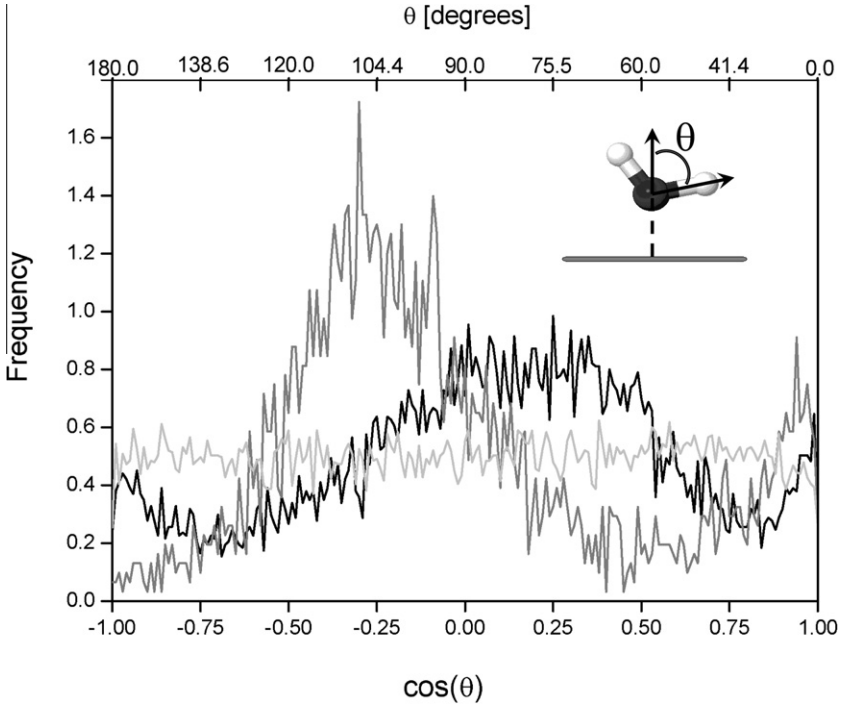

Fig. 7. Distribution of $\cos\theta$ for Layer 1 (black line), Layer 2 (dark gray) and bulk (light gray) regions around the graphene sheet. We also include an upper axis to help read the corresponding value of the angle.

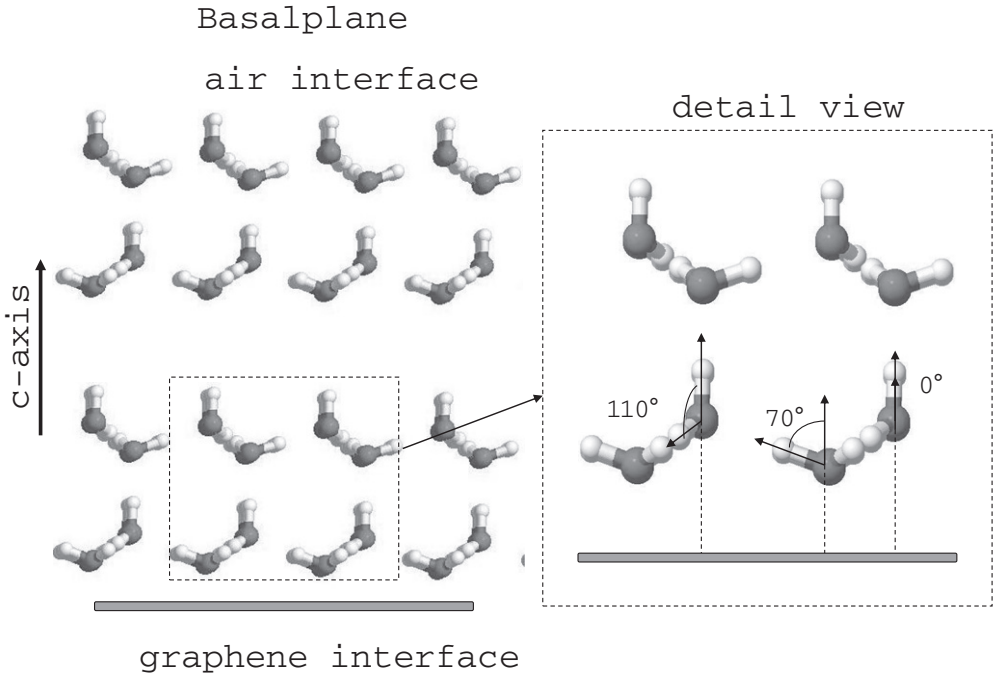

Fig. 8. Scheme of the structure of ice Ih, indicating the surfaces compatible with the (more disordered) local arrangements that tend to grow at the water/graphene and the water/air interfaces. In the detailed view we indicate the θ angles typical for molecules in Layer 1 (70°) and for molecules in Layer 2 (0° and 110°).

(T = 240 K, that is, within the supercooled regime when water gets more structured) which shows sharper peaks and a more pronounced peak separation. At such temperature, the separation between the first and second coordination shells increases significantly (and the fifth neighbor of the surface water molecules move to larger distances form the central molecule). This lowering in the local density significantly favors local structuring. As regards the structural order increase in the vicinal water molecules as we move from the smallest radius nanotube to the largest one and the graphene sheet, this is also related to a local density decrease that favors water ordering and orientation. In all cases the first three neighbors of the water molecules lay well within 3 Å of the central molecule (a distance that enables good hydrogen bond formation) while the fourth neighbor is placed roughly at 3.2 Å. For the nanotubes with radii smaller than 10 Å the fifth neighbor is located at roughly 3.5 Å while this distance grows to roughly 3.6 Å for the nanotubes with nanometric radii and for the graphene sheet. Again, this density lowering favors a local structuring where the OH bonds tend to be in plane with the surface or normal to it, as we shall see in the following subsection.

3.2. Hydrogen bonding and orientational ordering of surface water molecules. Tendency for ice Ih-like structuring

In this section we shall examine the hydrogen bonding and orientation of the water molecules close to the graphene sheet and the nanotube surfaces. In order to find hydrogen bonds (HBs) we used a geometric criterion (shown in past studies [37,35,34] to provide reasonable results also consistent with more elaborated criteria): A HB implies an O–O distance of less than 3.5 Å and an angle O–H... O lower than 30°. In Fig. 6(a) we display the distribution of distances Z to the graphene plane of the molecules that lie within 2.5 and 4.25 Å of the surface (that is, for molecules within the first peak of the density profile of Fig. 5), by discriminating between the ones that participate in four or more HBs and those ones which form three or less (we present the curve for a low temperature of T = 240 K in order to get clearer results but similar ones are obtained at ambient temperature). From this graph we can see that this region is basically the product of two different regions (the first and the second hydration layers) which from now on we shall call (hydration) Layer 1 and (hydration) Layer 2. Layer 1, which extends between 2.5 and 3.5 Å (roughly the crossing point in Fig. 6(a)) is mostly populated by molecules with three HB partners, while Layer 2, extending between 3.5 and 4.25 Å comprises molecules with preferentially four HBs, as can be seen in Fig. 6(b).

In order to better determine the structuring of these two first hydration layers, we studied the orientation of the water molecules comprised in each of them. In Fig. 7 we present this study for Layers 1 and 2 and also for bulk layers in the case of the graphene sheet. We plot the probability of $cos(\theta)$, where θ is the angle formed by the OH bonds of the water molecules with the normal to the graphene sheet. This quantity is interesting since it is amenable of comparison with experimental surface sum-frequency vibrational spectroscopy data [15], when available. From such a figure we can learn that the molecules in Layers 1 and 2 have clear preferential ordering, at variance from the situation for bulk water (also shown in the graph). Layer 1 shows a peak corresponding to angles of 70° while Layer 2 presents peaks for angles of 110° and 0°. This means that the molecules in Layer 1 tend to form HBs with that of Layer 2 (a fact we also verified by direct inspection and calculations), only forming 3 HBs due to the impossibility to complete the tetrahedron in the direction of the graphene layer. In turn, the molecules in Layer 2 also form HB with molecules in the second peak of the density profile (located at around 6 – 7 Å of the surface, cf. Fig. 5) with this HB aligned with the normal to the surface. This arrangement is typical of ice Ih, as can bee seen in the scheme of Fig. 8. Thus, this situation is similar to that of the water/air interface, but contrary to such case in which the molecules in the first hydration layer orient an OH bond towards the air [15,41], here the graphene surface impedes such orientation.

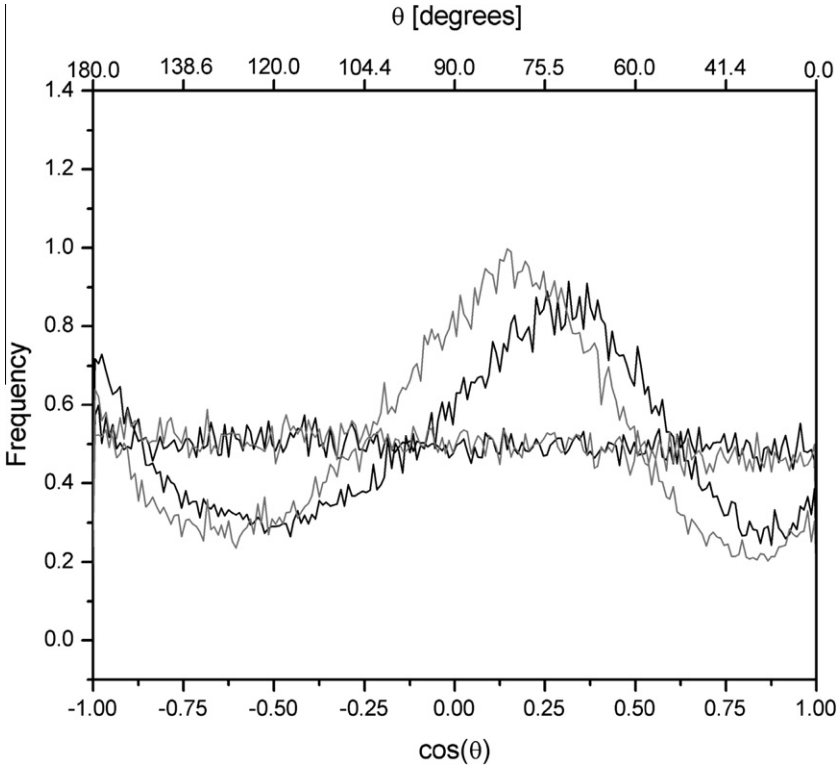

Fig. 9. Distribution of $cos\theta$ for Layer 1 and bulk layers around the nanotube of radius 67.5 Å (gray lines) and of the nanotube of radius 2.0 Å (black lines). In both cases the bulk layers are the ones that show no orientational preference.

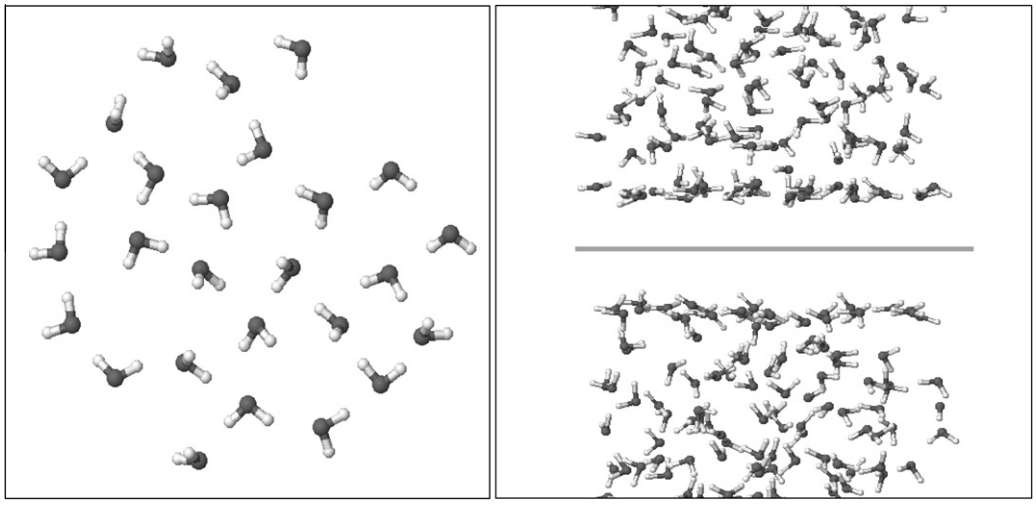

Fig. 10. Left: Top view of a typical configuration of the water molecules above the surface of the graphene sheet whose distance is closer than 4.25 Å to such surface. The graphene surface (not shown) is below these water molecules. Most of the OH bonds of the water molecules lie on a plane parallel to the graphene surface while some other OH bonds are oriented towards the observer (towards the bulk water). Right: Side view of the graphene sheet (seen as a line in the middle of the figure) with part of the solvating water molecules (a typical configuration). The same above-described tendency in the orientation of the water molecules is here evident.

Thus, around graphene the local ice Ih structure grows in the other direction along the c-axis of the basal plane: from bottom to top (please see the scheme) and not from top to bottom as is the case of the water/air interface [15,41]. This impediment for Layer 1 to orient an OH angle towards the graphene surface together with the impossibility to form four HBs excludes the fourth neighbors out of the surface to the second peak of the density profile (at $6-7$ Å from the surface). This gap in the density profile (clearly evidenced by the LSI index) makes this layer adopt a low local density arrangement necessary for the local formation of an ice Ih-like structure.

In Fig. 9 we display the $cos\theta$ for region 1 around the nanotube of radius 67.5 Å and of the nanotube of radius 2.0 Å. Here θ is the angle between the OH bond of the water molecule and the normal to the nanotube (the line perpendicular to the nanotube axis that passes through the oxygen atom of the corresponding molecule). Outer regions show no preferential orientation in both cases (data not shown). We can see that the orientation of the water molecules around region 1 of the large nanotube is similar to that of the graphene sheet (similar peak positions). For the small nanotube the distribution displays a slightly lower peak, thus showing that while there is a tendency to be oriented in a similar way, the water molecules are slightly less oriented than in the case of the large nanotube. Again, the non-extended and highly curved nature of this surface makes the proximal water molecules (mostly mutually hydrogen bonded) to be less ordered.

In order to illustrate the structural arrangement and orientation of the water molecules proximal to an extended hydrophobic surface we show a typical configuration of the water molecules close to the graphene sheet. We plot water molecules that are closer than 4.25 Å to the surface (Layers 1 and 2 comprising the first peak in the density profile). Fig. 10 shows a side view of this region over the graphene sheet together with a top view of the water molecules above the graphene sheet. We can clearly observe that the water molecules tend to orient an OH bond parallel to the surface and also that some OH are oriented towards the bulk water. Additionally, we can see that the water molecules of this region show a strong tendency to form hydrogen bonds between them and in some cases with water molecules of the upwards region. The existence of a considerable gap or local density depletion after around 4.25 Å is also evident. Thus, even when at ambient temperature thermal fluctuations tend to introduce disorder in this region, a tendency to ice Ih local ordering is manifest.

4. Conclusions

In this work we have studied the structure and orientation of water molecules around model graphitic-like hydrophobic surfaces. We have focused on the role of geometry by moving from a flat graphene sheet to carbon nanotubes of different radii and fullerenes (by studying their outer or convex surface). For the graphene sheet and the large radii nanotubes the water molecules proximal to the surface have been shown to be far more structured and oriented than the bulk, orienting their OH bonds parallel to the hydrophobic surface (in plane) and towards the bulk water region (normal to the graphene plane). The lack of one hydrogen bond in the direction towards the surface makes the water molecules to lower their local density by excluding their fourth neighbor and their second coordination shell, a fact that helps improve their local order and their orientation. In this sense, the first hydration layers of graphene show a clear tendency to arrange in a local structure resembling ice Ih. This ice-like structure is adopted by the first two or three water layers and grows following the *c* axis of the basal plane of ice Ih but in the other way as compared to the water/air interface. This is so since the water molecules adjacent to the surface resign a different kind of HB: in the case of the air/water interface this corresponds to a donor (thus orienting an OH bond towards the air) while in the cases studied here corresponds to an acceptor. However, this structuring and orientation is quickly lost as we move out of the surface towards the bulk. Additionally, we have shown that as the curvature of the surface increases (for example, as the radii of the nanotubes get smaller) this ordering of the proximal water begins to decrease smoothly whenever we deal with an extended surface. However, when the surface gets partially non-extended (nanotubes with subnanometric diameter) or completely non-extended (subnanometric diameter fullerenes) this structuring and orientation is quickly lost given the stringent geometrical constraints imposed by the surface.

Acknowledgments

Financial support from ANPCyT (both through a PICT grant and PME 2006-1581), MINCyT and CONICET is gratefully acknowledged. G.A.A., M.A.F., E.P.S. and L.M.A. are research fellows of CONICET. D.C.M. thanks CONICET and ANPCyT for a fellowship.

References

[1] D.M. Huang, D. Chandler, Proc. Natl. Acad. Sci. U.S.A. 97 (2000) 8324.
[2] X. Huang, C.J. Margulis, B.J. Berne, Proc. Natl. Acad. Sci. U.S.A. 100 (2003) 11953.
[3] A. Bizzarri, S. Cannistraro, J. Phys. Chem. B 106 (2002) 6617.
[4] D. Vitkup, D. Ringe, G.A. Petsko, M. Karplus, Nat. Struct. Biol. 7 (2000) 34.
[5] N. Choudhury, B. Montgomery Pettitt, J. Phys. Chem. B 109 (2005) 6422.
[6] H.E. Stanley, P. Kumar, L. Xu, Z. Yan, M.G. Mazza, S.V. Buldyrev, S.-H. Chen, F. Mallamace, Physica A 386 (2007) 729.
[7] N. Giovambattista, P.G. Debenedetti, C.F. Lopez, P.J. Rossky, Proc. Natl. Acad. Sci. USA 105 (2008) 2274.
[8] N. Nandi, B. Bagchi, J. Phys. Chem. B 101 (1997) 10954.
[9] C. -Y. Lee, J.A. McCammon, P.J. Rossky, J. Chem. Phys. 80 (1994) 3334;
S.H. Lee, P.J. Rossky, J. Chem. Phys. 100 (1984) 4448.
[10] M. Maccarini et al., Langmuir 23 (2007) 598.
[11] P. Kumar, S.V. Buldyrev, F.W. Starr, N. Giovambattista, H.E. Stanley, Phys. Rev. E 72 (2005) 051503.
[12] P. Gallo, M. Rovere, Phys. Rev. E 76 (2007) 061202.
[13] T.G. Lombardo, N. Giovambattista, P.G. Debenedeti, Faraday Discuss. 141 (2009) 359.
[14] D.C. Malaspina, E.P. Schulz, L.M. Alarcón, M.A. Frechero, G.A. Appignanesi, Eur. Phys. J. E 32 (2010) 35.
[15] Y.R. Shen, V. Ostroverkhov, Chem. Rev. 106 (2006) 1140.
[16] G. Hummer, J.C. Rasaiah, J.P. Noworyta, Nature 414 (2001) 188.
[17] A. Alexiadis, S. Kassinos, Chem. Rev. 108 (2008) 5014.
[18] J.C. Rasaiah, S. Garde, G. Hummer, Ann. Rev. Phys. Chem. 59 (2008) 713.
[19] W.L. Jorgensen, J. Chandrasekhar, J.D. Madura, R.W. Impey, M.L. Klein, J. Chem. Phys. 79 (1983) 926.
[20] M.W. Mahoney, W.L. Jorgensen, J. Chem. Phys. 112 (2000) 8910.
[21] H.J.C. Berendsen, J.P.M. Postma, W.F. van Gunsteren, A. DiNola, J.R. Haak, J. Chem. Phys. 81 (1984) 3684.
[22] D.A. Case, T.A. Darden, I.T.E. Cheatham, C.L. Simmerling, J. Wang, R.E. Duke, R. Luo, K.M. Merz, D.A. Pearlman, M. Crowley, R.C. Walker, W. Zhang, B. Wang, S. Hayik, A. Roitberg, G. Seabra, K.F. Wong, F. Paesani, X. Wu, S. Brozell, V. Tsui, H. Gohlke, L. Yang, C. Tan, J. Mongan, V. Hornak, G. Cui, P. Beroza, D.H. Mathew, C. Schafmeister, W.S. Ross, P.A. Kollman, AMBER9, University of California, San Francisco, CA, 2006;
T. Darden, D. York, L. Pedersen, J. Chem. Phys. 98 (1993) 10089;
U. Essmann, L. Perera, M.L. Berkowitz, T. Darden, H. Lee, L.G. Pedersen, J. Chem. Phys. 103 (1995) 8577;
M.F. Crowley, T.A. Darden, T.E. Cheatham, D.W. Deereld II, J. Supercomput. 11 (1997) 255;
C. Sagui, T.A. Darden, in: L.R. Pratt, G. Hummer (Eds.), Simulation and Theory of Electrostatic Interactions in Solution, American Institute of Physics, Melville, NY, 1999, p. 104113;
J. Wang, R.M. Wolf, J. Caldwell, P.A. Kollman, D.A. Case, J. Comput. Chem. 25 (2004) 1157;;
V. Hornak, R. Abel, A. Okur, B. Strockbine, A. Roitberg, C. Simmerling, Proteins: Struct. Funct. Bioinform. 65 (2006) 712.
[23] P.G. Debenedetti, Metastable Liquids, Princeton University Press, Princeton, NJ, 1996.
[24] O. Mishima, H.E. Stanley, Nature 396 (1998) 329.
[25] C.A. Angell, Chem. Rev. 102 (2002) 2627.
[26] C.A. Angell, Ann. Rev. Phys. Chem. 55 (2004) 559.
[27] E. Shiratani, M. Sasai, J. Chem. Phys. 104 (1996) 7671.
[28] E. Shiratani, M. Sasai, J. Chem. Phys. 108 (1998) 3264.
[29] O. Mishima, L.D. Calvert, E. Whalley, Nature 310 (1984) 393.
[30] H.-G. Heide, Ultramicroscopy 14 (1984) 271.
[31] T. Loerting, C. Salzmann, I. Kohl, E. Mayer, A. Hallbrucker, Phys. Chem. Chem. Phys. (Incorporating Faraday Transactions) 3 (2001) 5355.
[32] T. Loerting, N. Giovambattista, J. Phys.: Condensed Matter 18 (2006) 919.
[33] F. Sciortino, H. Geiger, H.E. Stanley, Phys. Rev. Lett. 65 (1990) 3452.
[34] J.A. Rodriguez Fris, G.A. Appignanesi, E. La Nave, F. Sciortino, Phys. Rev. E 75 (2007) 041501.
[35] G.A. Appignanesi, J.A. Rodriguez Fris, F. Sciortino, Eur. Phys. J. E 29 (2009) 305.
[36] J.R. Errington, P.G. Debenedetti, Nature 409 (318) (2001).
[37] D.C. Malaspina, J.A. Rodríguez Fris, G.A. Appignanesi, F. Sciortino, Europhys. Lett. 88 (2009) 16003.
[38] G.A. Appignanesi, J.A. Rodríguez Fris, R.A. Montani, W. Kob, Phys. Rev. Lett. 96 (2006) 057801.
[39] G.A. Appignanesi, J.A. Rodríguez Fris, M.A. Frechero, Phys. Rev. Lett. 96 (2006) 237803.
[40] G.-J. Guo, Y.-G. Zhang, M. Li, C.-H. Wu, J. Chem. Phys. 128 (2008) 194504.
[41] Y. Fan, X. Chen, L. Yang, P.S. Cremer, Y.Q. Gao, J. Phys. Chem. B 113 (2009) 11672.